

# Dependence of $\text{PbMoO}_4$ crystal damage threshold on $\text{Nd}^{3+}$ concentration and method of doping

*V.N.Baumer, Yu.N.Gorobets, L.V.Gudzenko, M.B.Kosmyna, B.P.Nazarenko, V.M.Puzikov, A.N.Shekhovtsov, Z.V.Shtitelman*

Institute for Single Crystals, STC "Institute for Single Crystals",  
National Academy of Sciences of Ukraine,  
60 Lenin Ave., 61001 Kharkiv, Ukraine

*Received June 29, 2010*

$\text{PbMoO}_4:\text{Nd}^{3+}$  crystals with the activator concentration up to 3 wt.% were grown by the Czochralski method. The damage threshold and incorporation coefficient dependences on the activator concentration and the method of doping were determined. The internal stress concentrations in  $\text{PbMoO}_4:\text{Nd}^{3+}$  crystals were estimated by means of optical polarization method.

Кристаллы  $\text{PbMoO}_4:\text{Nd}^{3+}$  с концентрацией активатора до 3 мас.% выращены методом Чохральского. Определены коэффициент вхождения и лучевая прочность в зависимости от концентрации активатора и метода его введения. Уровень внутренних напряжений в кристаллах  $\text{PbMoO}_4:\text{Nd}^{3+}$  оценен при помощи оптического поляризационного метода.

## 1. Introduction

To expand the laser generation band, the effect of stimulated Raman scattering (SRS) in solids can be successfully applied [1]. The use of active laser media combining the laser generation function and SRS-conversion makes it possible to simplify the laser design and raise the laser system efficiency. It is known that lead tungstate  $\text{PbWO}_4$  (PWO) and lead molybdate  $\text{PbMoO}_4$  (PMO) single crystals with scheelite-type structure (sp.gr.  $I4_1/a$ ) possess the maximum SRS integral intensities among the crystals with different quasi-molecular anions [1, 2]. This fact should provide high SRS conversion efficiency and  $\sim 900 \text{ cm}^{-1}$  shift of the laser wavelength caused by interaction of laser active ion generation with the vibration modes of  $(\text{WO}_4)^{2-}$  or  $(\text{MoO}_4)^{2-}$  anions.

In [3] laser and self-Raman laser generations in  $\text{PMO}:\text{Nd}^{3+}$  crystal were obtained under 1.5 W laser diode (LD) pumping.

Thereat, the self-Raman output pulse energy was equal to 6  $\mu\text{J}$  (1<sup>st</sup> Stokes component,  $\lambda = 1163 \text{ nm}$ ) at 500 ps pulse duration. To generate the Stokes components effectively, much higher pumping power should be applied. Therefore, in the present study we investigated the radiation damage threshold of  $\text{PMO}:\text{Nd}^{3+}$  crystals depending on the concentration of  $\text{Nd}^{3+}$  and the doping method.

## 2. Experimental

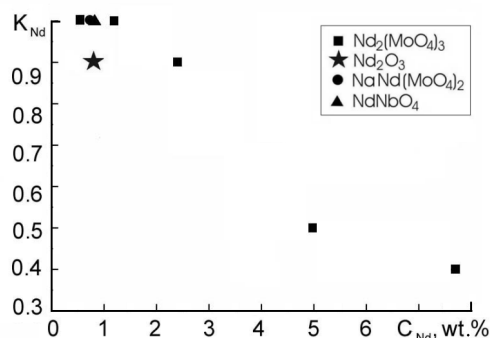
Pure and  $\text{Nd}^{3+}$ -doped PMO single crystals were grown in air from 100  $\text{cm}^3$  and 500  $\text{cm}^3$  Pt-crucibles by the Czochralski method using the "Analog" automatic set-up equipped with a weight control system. The crystals were grown onto a seed oriented along the direction [001]. This direction was chosen due to a cylindrical morphology of crystal and a simple production procedure of oriented sample. The growth

Table 1. Time-temperature conditions of solid state synthesis

Sample	Temperature, °C	Duration, h	Phase content, wt. %
PbMoO <sub>4</sub>	650	10	97±2
NaNd(MoO <sub>4</sub> ) <sub>2</sub>	650	10	96±2
Nd <sub>2</sub> (MoO <sub>4</sub> ) <sub>3</sub>	800	10	95±2
NdNbO <sub>4</sub>	1100	10	96±2

parameters for all the crystals were: the temperature gradient  $T_z = 50-70$  deg/cm, the rotation rate  $\omega = 20-30$  min<sup>-1</sup>, the pulling rate  $V_z = 1-3$  mm/h. The variation of growth parameters in these ranges allowed us to grow PMO crystals up to 40 mm and a length up to 150 mm. The PMO crystals chosen for investigation were of up to 25 mm in diameter and up to 50 mm long. All PMO crystals to be investigated were grown under the same conditions (at fixed values of temperature gradient, rotation and pulling rates). In our experiments the value  $H/D$  (ratio of height of crystal cone to diameter of crystal) was  $\sim 0.25$ . All the crystals were free of impurity phases and macroscale defects (gas bubbles, crystal cracking). The pure crystals had a yellowish color, Nd<sup>3+</sup> doped crystals were lilac. The color intensity of doped PMO crystals depended on Nd<sup>3+</sup> concentration.

To dope PMO crystals, we used Nd<sub>2</sub>O<sub>3</sub>, as well as presynthesized Nd<sub>2</sub>(MoO<sub>4</sub>)<sub>3</sub>, NaNd(MoO<sub>4</sub>)<sub>2</sub> and NdNbO<sub>4</sub> compounds. When Nd<sub>2</sub>O<sub>3</sub> and NdNbO<sub>4</sub> compounds were used, the ratio PbO/MoO<sub>3</sub> in the PMO melt was stoichiometric, while with Nd<sub>2</sub>(MoO<sub>4</sub>)<sub>3</sub> and NaNd(MoO<sub>4</sub>)<sub>2</sub> the PMO melt was enriched with MoO<sub>3</sub>. The starting chemical reagents were: PbO, Nb<sub>2</sub>O<sub>5</sub>, Na<sub>2</sub>CO<sub>3</sub> and Nd<sub>2</sub>O<sub>3</sub> — 99.99 %, MoO<sub>3</sub> — 99.95 %. The synthesis of PMO and dopants was carried out according to the ceramic technology. The stoichiometric blend of starting reagents was heated to the defined temperature and kept for the defined time. The temperature-time regimes of the solid state synthesis are presented in Table 1. The X-ray structure studies were carried out on a SIEMENS D500 automated diffractometer in CuK<sub>α</sub> radiation ( $\lambda = 1.5418$  Å, graphite monochromator) using the  $2\theta/\theta$  scanning method at rates 0.24 grad/min. The incorporation coefficient  $K_{Nd}$  was calculated as ratio of Nd concentration in crystal to Nd concentration in melt.

Fig. 1. Dependences of the  $K_{Nd}$  on Nd concentration in the PbMoO<sub>4</sub> melt.

The content of Nd<sup>3+</sup> in PMO crystals was determined by means of inductively coupled plasma analysis (PRACE SCAN Advantage spectrometer). To determine Nd<sup>3+</sup> concentration in PMO:Nd<sup>3+</sup> crystals, a specimen was cut off from central part of every ingot. The damage threshold and internal stresses were studied on oriented polished 10×10×10 mm<sup>3</sup> crystal samples produced from the central cylindrical part of each crystal. Under He-Ne laser beam passing through a sample no scattering was observed. In the first instance the axial angle had been measured, hereafter the same samples were used for the damage threshold definition.

To determine the damage threshold, YAG:Nd<sup>3+</sup> pulsed laser ( $\lambda = 1.06$  μm, TEM<sub>00</sub>-mode, 10 ns pulse duration, 1 Hz repetition rate, the spot diameter  $\sim 45$  μm, Gaussian distribution of intensity) was used.

The axial angle  $2V$  was measured by means of optical polarization method using a MIN-8 polarizing microscope according to the procedure described in [4]. The instrument magnification was 70.5. The said angle was determined for every sample as the average for three points located on the plane (001).

### 3. Results and discussion

For total absorption of LD pumping energy, heavy Nd<sup>3+</sup>-doped laser active media are required. Therefore, we investigated the dependence of  $K_{Nd}$  value on the activator concentration in the PMO melt and the doping method. To grow Nd<sup>3+</sup> doped PMO crystals, isostructural (Nd<sub>2</sub>(MoO<sub>4</sub>)<sub>3</sub>, NaNd(MoO<sub>4</sub>)<sub>2</sub>) and non-isostructural (Nd<sub>2</sub>O<sub>3</sub>, NdNbO<sub>4</sub>) compounds were used, as well as charge-compensating ions Na<sup>+</sup> (NaNd(MoO<sub>4</sub>)<sub>2</sub>) and Nb<sup>5+</sup>

(NdNbO<sub>4</sub>). The  $K_{Nd}$  concentration dependence is presented in Fig. 1.

As seen from Fig. 1,  $K_{Nd} \sim 1$  for the concentrations up to  $\sim 1$  wt.%. An exception is Nd<sub>2</sub>O<sub>3</sub> case, where  $K_{Nd} \sim 0.9$ . At further increase of the Nd concentration in the melt the coefficient  $K_{Nd}$  is decreased (Nd<sup>3+</sup> doping by means of Nd<sub>2</sub>(MoO<sub>4</sub>)<sub>3</sub>).

According to [5, 6], the system PbMoO<sub>4</sub>-Nd<sub>2</sub>(MoO<sub>4</sub>)<sub>3</sub> contains the solid solutions in the whole concentration range. By comparing the ionic radii of Pb<sup>2+</sup> (1.26 Å) and Nd<sup>3+</sup> (0.99 Å) one can assume that the coefficient  $K_{Nd}$  will be approximately  $\sim 1$ . However, as seen from Fig. 1, the decrease of  $K_{Nd}$  in PMO crystals begins from  $\sim 1$  wt.% in the melt, and at 7.7 wt.% the coefficient is equal to 0.4.

The coefficients  $K_{Na}$  and  $K_{Nb}$  were not determined. But according to the data of X-ray analysis the parameters of PMO:Nd<sup>3+</sup> unit cell are different under the same Nd concentrations at use of Nd<sub>2</sub>(MoO<sub>4</sub>)<sub>3</sub>, NaNd(MoO<sub>4</sub>)<sub>2</sub> and NdNbO<sub>4</sub> compounds (Table 2). This fact allows us to conclude that Na<sup>+</sup> and Nb<sup>5+</sup> build in PMO crystal lattice too.

Our measurements of the damage threshold show that the maximum value of optical breakdown  $J_{Th} \sim 90$  J/cm<sup>2</sup> is achieved at use of Nd<sub>2</sub>O<sub>3</sub> (the concentration of Nd<sup>3+</sup> in the crystal is 0.8 wt.%, Fig. 2). It should be noted that in the case of Nd<sub>2</sub>(MoO<sub>4</sub>)<sub>3</sub> introduction (the Nd<sup>3+</sup> concentration in the crystal is 0.8 wt.%) the damage threshold  $J_{Th} \sim 60$  J/cm<sup>2</sup> is close to that of a pure PMO crystal. Co-doping with Nb<sup>5+</sup> does not affect the damage threshold value dramatically: under such conditions —  $J_{Th} \sim 58$  J/cm<sup>2</sup>, but the use of Na<sup>+</sup> practically halves the magnitude of optical breakdown: in this case  $J_{Th} \sim 29$  J/cm<sup>2</sup>. At further growth of the Nd concentration in PMO crystal the damage threshold  $J_{Th}$  is decreased.

There are few types of physical effects leading to the optical breakdown. The first one is conditioned by the interaction of

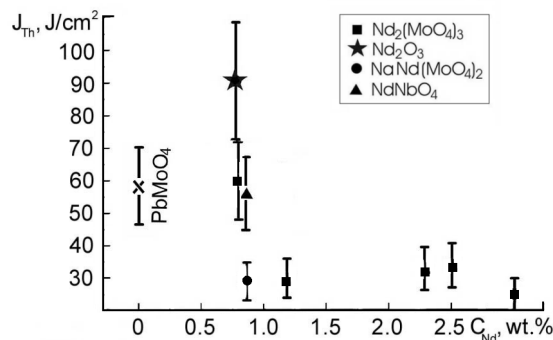


Fig. 2. Dependences of the damage threshold  $J_{Th}$  on Nd concentration in the PbMoO<sub>4</sub> crystal.

laser radiation with impurities or absorbing inclusions. The next one is connected with nonlinear effects (self-focusing, multiphoton absorption), when the space-time distortion of laser radiation is going on in a dielectric crystal. The last effect, self laser induced breakdown happens when the space-time distortion of laser radiation is not in a crystal [7]. On one hand the damage threshold will be a result of laser radiation absorption by impurities, but on other hand impurities are able to improve the optical breakdown dramatically by means of electron trap forming [8]. At further growth of impurity content in a crystal the probability of phase inclusion forming or other absorbing heterogeneity forming is increased and the damage threshold is decreased.

As it was shown in [9, 10] the anionic group (WO<sub>4</sub>)<sup>2-</sup> is kept in melts of simple and double sheelite like tungstates. In our case we can suppose that at use of Nd<sub>2</sub>(MoO<sub>4</sub>)<sub>3</sub> and NaNd(MoO<sub>4</sub>)<sub>2</sub> compounds the anionic groups (MoO<sub>4</sub>)<sup>2-</sup> are kept in melt too. At the same time the use of Nd<sub>2</sub>O<sub>3</sub> leads to the O<sup>2-</sup> containing melt. Thus, the use of different compounds for Nd doping can affect structure of melt and predetermine an activator center structure.

According to the hypothesis proposed in [11] on the base of dielectric response measurements of PWO:Nd<sup>3+</sup> crystals, at low Nd<sup>3+</sup> concentrations these ions build in the Pb<sup>2+</sup>

Table 2. Parameters of the PbMoO<sub>4</sub>:Nd unit cell at use of different dopants

Parameter	Compound; Nd concentration in the crystal, wt.%				
	Pure	Nd <sub>2</sub> O <sub>3</sub> ; 0.75	Nd <sub>2</sub> (MoO <sub>4</sub> ) <sub>3</sub> ; 0.8	NaNd(MoO <sub>4</sub> ) <sub>2</sub> ; 0.8	NdNbO <sub>4</sub> ; 0.8
$a$ , Å	5.43641(8)	5.43394(3)	5.43389(4)	5.43099(4)	5.43386(4)
$c$ , Å	12.10786(9)	12.10095(11)	12.10049(13)	12.08866(12)	12.08813(12)
$V$ , Å <sup>3</sup>	357.844(4)	357.313(5)	357.293(5)	356.563(5)	356.925(5)

sublattice and form  $(2\text{Nd}_{\text{Pb}}^{3+})^{\bullet} - (\text{V}_{\text{Pb}})^{\prime\prime}$  activator center, the excessive positive charge being compensated by lead vacancy. In heavily Nd<sup>3+</sup> doped PMO crystals more sophisticated activator center  $(\text{Nd}_{\text{W}}^{3+})^{\prime\prime\prime} - (\text{Nd}_{\text{Pb}}^{3+})^{\bullet} - (\text{V}_{\text{O}})^{\bullet\bullet}$  is formed; thereat Nd<sup>3+</sup> is built in the Pb<sup>2+</sup> and W<sup>6+</sup> sublattices, the excessive negative charge is compensated by oxygen vacancy. In all the cases the PMO crystals reported in [11] were doped with Nd<sub>2</sub>O<sub>3</sub>. Obviously, a structure of Nd<sup>3+</sup> activator center will be determined by a crystallographic position of Nd<sup>3+</sup> ion in PMO lattice and charge compensating defect and will depend on Nd concentration and method of doping.

The presence of internal stresses in the crystal which are induced by crystal growth technology and impurities may considerably affect the magnitude of optical breakdown. The absorption of laser radiation by absorbing heterogeneity leads to the heating of local region with following extension. This is caused by the fact that under irradiation of the crystal with nanosecond laser pulses, the mechanism of crystal cracking connected with accumulation of thermo-elastic stresses, is realized [12, 13].

Therefore, we estimated the level of structure perfection from the distortion of isogyres in the interference pattern observed at passage of polarized light along the direction [001]. Internal stresses give rise to anomalous biaxiality in the crystal, and the axial angle 2V is proportional to the level of these stresses. So, we measured the axial angle 2V for all the doped and co-doped PMO crystals using the optical polarization method. The obtained data are presented in Fig. 3.

The pure and Nd<sup>3+</sup> containing PMO crystals (<1 wt. %) where isostructural compounds (Nd<sub>2</sub>(MoO<sub>4</sub>)<sub>3</sub>, NaNd(MoO<sub>4</sub>)<sub>2</sub>) were used, are characterized by the minimum magnitudes of 2V angle varying between 27' and 32'. The introduction of the non-isostructural compounds (Nd<sub>2</sub>O<sub>3</sub>, NdNbO<sub>4</sub>) in the PMO melt raises the value of 2V angle up to 43'–47'. At further increase of Nd<sup>3+</sup> concentration in the PMO crystal internal stresses grow. The heavily doped PMO crystal (3 wt.%) showed the maximum magnitude of 2V angle — 1°2'.

Note that the PMO:Nd<sup>3+</sup> crystals with the highest level of internal stresses at <1 wt.% concentrations of the activator possess the maximum magnitudes of damage threshold, too. Therefore, the most

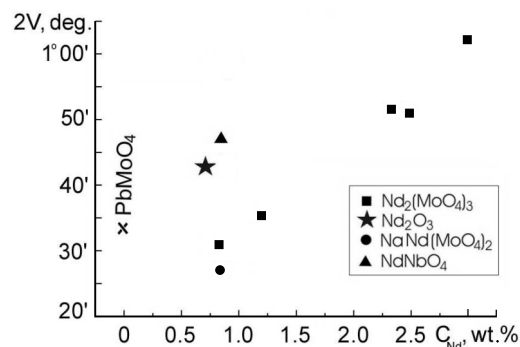


Fig. 3. Dependences of the axial angle 2V on Nd concentration in the PbMoO<sub>4</sub> crystal.

probable factor which causes optical breakdown in PMO:Nd<sup>3+</sup> crystals at these concentrations may be the compensating excessive charge defect.

#### 4. Conclusion

PbMoO<sub>4</sub>:Nd<sup>3+</sup> crystals with the activator concentration up to 3 wt.% were grown by the Czochralski method. Few doping methods (Nd introduction in the form of isostructural and non-isostructural compounds, co-activation) were used. It was shown, that incorporation coefficient  $K_{\text{Nd}}$  equals to ~1 for the concentrations up to ~1 wt.% at the use of Nd<sub>2</sub>(MoO<sub>4</sub>)<sub>3</sub>, NaNd(MoO<sub>4</sub>)<sub>2</sub> and NdNbO<sub>4</sub> dopants. An exception is Nd<sub>2</sub>O<sub>3</sub> case, where  $K_{\text{Nd}} \sim 0.9$ . At further increase of the Nd concentration in the melt at Nd<sub>2</sub>(MoO<sub>4</sub>)<sub>3</sub> doping the coefficient  $K_{\text{Nd}}$  is decreased.

The damage threshold was studied depending on the activator concentration and the method of doping too. It was established that the maximum magnitude of damage threshold 90 J/cm<sup>2</sup> was achieved at 0.75 wt.% Nd concentration in the PMO crystal. Thus from practical view point the use of Nd<sub>2</sub>O<sub>3</sub> for PMO doping is more effectual because of simpler procedure of PMO:Nd<sup>3+</sup> crystal production (there is no necessity of compound synthesis for doping) and high magnitude of the damage threshold. The level of structure perfection of PMO:Nd<sup>3+</sup> crystals was estimated by means of axial angle 2V measurements.

*Acknowledgements.* The authors are grateful Dr. I.S.Voronina (A.Prokhorov General Physics Institute, RAS) for useful discussion concerning determination of the axial angle 2V.

**References**

1. T.T.Basiev, M.E.Doroshenko, L.I.Ivleva et al., *Quan. Electron.*, **36**, 720 (2006).
2. T.T.Basiev, A.A.Sobol, Yu.K.Voronko et al., *Opt. Mater.*, **15**, 205 (2000).
3. T.T.Basiev, S.V.Vassiliev, M.E.Doroshenko et al., *Opt. Lett.*, **31**, 65 (2006).
4. A.G.Shtukenberg, Yu.O.Punin, *Optically Anomalous Crystals*, Springer, Dordrecht (2007).
5. V.P.Barzakovskiy, V.V.Lapin, A.I.Boykova et al., *Phase Diagrams of Silicate Systems*, Nauka, Leningrad (1974) [in Russian].
6. M.V.Mokhosoev, J.C.Bazarova, *Complex Oxide of Molybdenum and Tungsten with Elements of the I-IV groups*, Nauka, Moscow (1990) [in Russian].
7. D.A.Cremers, L.J.Radziemski, *Handbook of Laser-induced Breakdown Spectroscopy*, John Wiley&Sons, New York (2006).
8. J.Koppitz, O.F.Schirmer, M.Wohlecke et al., *Ferroelectrics*, **92**, 233 (1989).
9. Yu.K.Voron'ko, A.A.Sobol', S.N.Ushakov et al., *Inorg. Mater.*, **36**, 947 (2000).
10. Yu.K.Voron'ko, A.A.Sobol', *Inorg. Mater.*, **41**, 420 (2005).
11. Weifeng Li, Hongwei Huang, Xiqi Feng, *Phys. Stat. Sol. (a)*, **202**, 2531 (2005).
12. A.A.Manenkov, A.M.Prokhorov, *Uspekhi Fiz.*, **29**, 104 (1986).
13. S.G.Kazantsev, *Quant. Electron.*, **24**, 263 (1997).

## **Залежність променевої стійкості кристалів PbMoO<sub>4</sub> від концентрації Nd<sup>3+</sup> та способу активування**

**В.М.Баумер, Ю.М.Горобець, Л.В.Гудзенко, М.Б.Космина,  
Б.П.Назаренко, В.М.Пузіков, О.М.Шеховцов, З.В.Штительман**

Кристали з концентрацією активатора до 3 мас.% вирощено методом Чохральського. Визначено коефіцієнт входження та променеву стійкість в залежності від концентрації активатора та метода його введення. Рівень внутрішніх напружень у кристалах PbMoO<sub>4</sub>:Nd<sup>3+</sup> оцінено за допомогою оптичного поляризаційного методу.